

Magnetic Interactions in $\text{Ge}_{1-x}\text{Cr}_x\text{Te}$ Semimagnetic Semiconductors

L. Kilanski,^{1, a)} A. Podgórní,¹ W. Dobrowolski,¹ M. Górská,¹ B. J. Kowalski,¹ A. Reszka,¹
 V. Domukhovski,¹ A. Szczerbakow,¹ K. Szałowski,² J. R. Anderson,³ N. P. Butch,^{3, b)}
 V. E. Slynko,⁴ and E. I. Slynko⁴

¹⁾*Institute of Physics, Polish Academy of Sciences, al. Lotnikow 32/46,
 02-668 Warsaw, Poland*

²⁾*Department of Solid State Physics, University of Łódź, ul. Pomorska 149/153,
 90-236 Łódź, Poland*

³⁾*Department of Physics and Center for Nanophysics and Advanced Materials,
 University of Maryland, College Park, MD 20742, USA*

⁴⁾*Institute of Materials Science Problems, Ukrainian Academy of Sciences,
 5 Wilde Street, 274001 Chernovtsy, Ukraine*

(Dated: 7 January 2019)

We present the studies of magnetic properties of $\text{Ge}_{1-x}\text{Cr}_x\text{Te}$ diluted magnetic semiconductor with changeable chemical composition $0.016 \leq x \leq 0.061$. A spin-glass state (at $T \leq 35$ K) for $x = 0.016$ and 0.025 and a ferromagnetic phase (at $T < 60$ K) for $x \geq 0.030$ are observed. The long range carrier-mediated magnetic interactions are found to be responsible for the observed magnetic ordering for $x < 0.045$, while for $x \geq 0.045$ the spinodal decomposition of Cr ions leads to a maximum and decrease of the Curie temperature, T_C , with increasing x . The calculations based on spin waves model are able to reproduce the observed magnetic properties at a homogeneous limit of Cr alloying, e.g. $x < 0.04$, and prove that carrier mediated Ruderman-Kittel-Kasuya-Yosida (RKKY) interaction is responsible for the observed magnetic states. The value of the Cr-hole exchange integral, J_{pd} , estimated via fitting of the experimental results with the theoretical model, is in the limits $0.77...0.88$ eV.

PACS numbers: 72.80.Ga, 75.40.Cx, 75.40.Mg, 75.50.Pp

Keywords: semimagnetic-semiconductors; ferromagnetic-materials; magnetic-properties

^{a)}Electronic mail: kilan@ifpan.edu.pl

^{b)}Present address: Lawrence Livermore National Laboratory, 7000 East Avenue, Livermore, CA 94550, USA

I. INTRODUCTION

Diluted magnetic semiconductors (DMS) are a very important and intensively studied group of materials because of their possible application in spin electronics devices.^{1,2} The combination of magnetic ions and a semiconductor matrix allows an independent control of electrical and magnetic properties of DMS by many orders of magnitude via changes in the technological parameters of the growth or post growth treatment of the compound. DMS compounds are usually developed on the basis of a III-V or II-VI semiconductor matrix into which transition metal or rare earth ions are introduced on a level of several atomic percent.³⁻⁵

IV-VI based DMS, in particular $\text{Ge}_{1-x}\text{TM}_x\text{Te}$ alloys (TM - transition metal), possess many advantages over widely studied $\text{Ga}_{1-x}\text{Mn}_x\text{As}$. The carrier concentration and the amount of TM ions can be controlled independently. Moreover, the solubility of TM ions in GeTe is very high allowing growth of homogeneous $\text{Ge}_{1-x}\text{TM}_x\text{Te}$ solid solutions over a wide range of chemical composition. Itinerant ferromagnetism with the Curie temperatures as high as 167 K for $x = 0.5$ was observed in bulk $\text{Ge}_{1-x}\text{Mn}_x\text{Te}$ crystals.⁶ Recently, numerous papers were devoted to the studies of thin epitaxial $\text{Ge}_{1-x}\text{Mn}_x\text{Te}$ layers.⁷⁻⁹ Recent results show that the Curie temperature in $\text{Ge}_{1-x}\text{Mn}_x\text{Te}$ layers can be controlled in a wide range of values reaching a maximum of about 200 K.¹⁰ Apart from Mn-alloyed GeTe, a significant attention has been recently turned onto other transition-metal-alloyed GeTe based DMS,¹¹ since they also show itinerant ferromagnetism with relatively high Curie temperatures $T_C \leq 150$ K.¹²⁻¹⁴ The progress in the technology of growth of a $\text{Ge}_{1-x}\text{Cr}_x\text{Te}$ alloy resulted in obtaining a high Curie temperature reaching maximum of 180 K for $x \approx 0.06$.¹⁵ In contrast to the epitaxial layers, there seems to be no detailed study of magnetic behavior of bulk $\text{Ge}_{1-x}\text{Cr}_x\text{Te}$ crystals. Therefore, detailed studies of Cr-alloyed GeTe crystals are very important in making further development in this class of compounds.

In this paper we present studies of magnetic properties of $\text{Ge}_{1-x}\text{Cr}_x\text{Te}$ bulk crystals with chemical composition x varying between $0.016 \leq x \leq 0.061$. Our main goal was to show that the magnetic properties of the alloy can be tuned by means of changes in its chemical composition. The present work extends our preliminary studies (see Ref. 16) of low Cr-content $\text{Ge}_{1-x}\text{Cr}_x\text{Te}$ samples with $x \leq 0.025$ into higher Cr composition $0.035 \leq x \leq 0.061$, in which the magnetic order changed dramatically from a spin-glass freezing into ferromagnetic align-

TABLE I. Results of basic characterization of $\text{Ge}_{1-x}\text{Cr}_x\text{Te}$ samples performed at room temperature including chromium content x , lattice parameter a , angle of distortion α , electrical resistivity ρ_{xx} , carrier concentration n and mobility μ .

$x \pm \Delta x$	$a \pm \Delta a$ (Å)	$\alpha \pm \Delta\alpha$ (deg)	ρ_{xx} ($10^{-3} \Omega\cdot\text{cm}$)	n (10^{20} cm^{-3})	μ ($\text{cm}^2/(\text{V}\cdot\text{s})$)
0.016 ± 0.004	5.9847 ± 0.0003	88.44 ± 0.01	3.05 ± 0.01	2.4 ± 0.1	8.0 ± 0.1
0.025 ± 0.003	5.9845 ± 0.0002	88.44 ± 0.01	2.67 ± 0.01	2.6 ± 0.1	10.1 ± 0.1
0.035 ± 0.005	5.9837 ± 0.0004	88.41 ± 0.01	1.97 ± 0.01	2.9 ± 0.1	10.0 ± 0.1
0.045 ± 0.005	5.9829 ± 0.0003	88.38 ± 0.01	1.45 ± 0.01	3.0 ± 0.1	16.0 ± 0.1
0.059 ± 0.006	5.9829 ± 0.0002	88.38 ± 0.01	1.18 ± 0.01	3.1 ± 0.1	23.0 ± 0.1
0.061 ± 0.006	5.9820 ± 0.0003	88.38 ± 0.01	1.04 ± 0.01	3.3 ± 0.1	19.2 ± 0.1

32 ment. The present work extends our earlier results by the use of high field magnetometry.
 33 The experimental results are analyzed within the model based on spin waves theory. The
 34 theoretical results are able to reproduce the observed magnetic properties of the alloy for
 35 $x \leq 0.04$ and prove, that carrier mediated Ruderman-Kittel-Kasuya-Yosida (RKKY)¹⁷⁻¹⁹ in-
 36 teraction was responsible for the observed magnetic states of the studied $\text{Ge}_{1-x}\text{Cr}_x\text{Te}$ samples
 37 for $x < 0.04$. The spinodal decomposition of Cr ions leads to saturation and decrease of the
 38 Curie temperature, T_C , for $0.04 < x < 0.061$.

39 II. SAMPLE PREPARATION AND BASIC CHARACTERIZATION

40 Our $\text{Ge}_{1-x}\text{Cr}_x\text{Te}$ crystals were grown using the modified Bridgman method. The growth
 41 procedure was modified similarly to the inclined crystallization front method, proposed by
 42 Aust and Chalmers for improving the quality of bulk alumina crystals.²⁰ The presence of
 43 additional heating elements in the growth furnace created a radial temperature gradient
 44 in the growth furnace, changing the slope of the solid-liquid interface by about 15° . The
 45 proposed modifications improved the crystal homogeneity and allowed the reduction of the
 46 number of crystal blocks in the as-grown ingot from a few down to a single one.

47 The chemical composition of the samples was determined using the energy dispersive
 48 x-ray fluorescence technique (EDXRF). The chemical composition of the ingots grown by
 50 this method changed continuously along the direction of crystal growth. To minimize the

51 heterogeneity of the individual samples the as-grown crystals were cut perpendicular to
52 the growth direction into thin slices each with a thickness of about 1 mm. This ensured
53 the heterogeneity of the individual slices to be relatively small with a maximum value of
54 about $\Delta x \leq 0.006$, where Δx represents the variation of the amount of Cr in the slice.
55 The results of the EDXRF measurements showed that the chemical composition of crystals
56 changed continuously along the ingot from $x \simeq 0.012$ up to 0.065. From all the crystal slices
57 we selected the ones in which the relative chemical inhomogeneity was the smallest in the
58 whole series (chemical composition of the samples is gathered in Table I).

59 The structural characterization of $\text{Ge}_{1-x}\text{Cr}_x\text{Te}$ crystals was performed with the use of
60 standard powder x-ray diffraction (XRD) technique. The XRD measurements were done at
61 room temperature using Siemens D5000 diffractometer. The obtained diffraction patterns
62 were then analyzed using Rietveld refinement method to determine the lattice parameters
63 of each sample. The obtained results indicated that all the samples were single phase and
64 crystallized in the NaCl structure with rhombohedral distortion in (111) direction. The
65 lattice parameter a as well as the angle of distortion α obtained for $\text{Ge}_{1-x}\text{Cr}_x\text{Te}$ crystals
66 are gathered in Table I. The lattice parameters of the studied crystals are similar to the
67 values for pure GeTe, i.e., $a = 5.98 \text{ \AA}$ and $\alpha = 88.3^\circ$.²¹ The lattice parameter of $\text{Ge}_{1-x}\text{Cr}_x\text{Te}$
68 samples is a decreasing function of chromium content x . The monotonic and close to a
69 linear decrease of a with x is in accordance with the Vegard law, which is a clear signature
70 that the Cr ions are incorporated to a large extent into cation positions in the GeTe crystal
71 lattice. The $a(x)$ dependence can be fitted with a linear function $a(x) = 5.9857 - 0.055 \cdot x$. The
72 directional coefficient of the $a(x)$ function is about 3 times lower than the values reported in
73 the literature for $\text{Ge}_{1-x}\text{Mn}_x\text{Te}$ crystals.²² We believe that a large fraction of the chromium
74 ions in the studied samples do not occupy the substitutional positions in the cation sublattice.
75 We must therefore assume the presence of chromium ions in various charge states, which
76 might have significant effects on the electrical and magnetic properties of the alloy.

77 Scanning electron microscopy (SEM) was used to study chemical homogeneity of selected
78 $\text{Ge}_{1-x}\text{Cr}_x\text{Te}$ samples. Two techniques were used simultaneously: (i) field emission scanning
79 electron microscopy with the use of Hitachi SU-70 Analytical UHR FE-SEM and (ii) Thermo
80 Fisher NSS 312 energy dispersive x-ray spectrometer system (EDX) equipped with SDD-
81 type detector. The SEM employed with this device allowed us to make microscopic pictures
82 of the crystal surface. A series of measurements performed on different samples revealed the

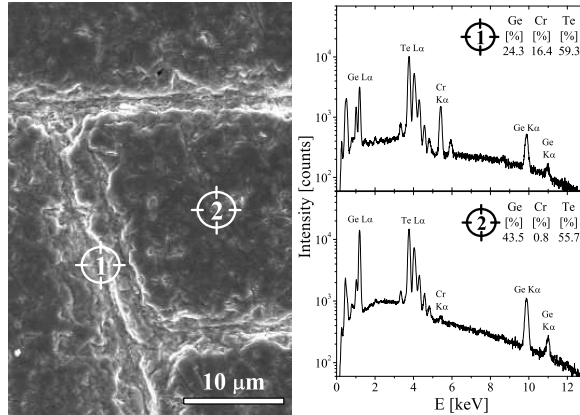


FIG. 1. SEM image of the surface of the selected $\text{Ge}_{0.941}\text{Cr}_{0.059}\text{Te}$ crystal and the EDS spectra measured at selected spots of the sample.

83 presence of a small concentration of pure Ge inclusions with diameters typically around a few
 84 micrometers inside the samples. However, since there was no signature of chromium in the
 85 observed Ge inhomogeneities, we believe that they should not affect magnetic properties of
 86 the studied crystals. No signature of chromium clustering was observed (within the limits of
 87 accuracy of the method) in the case of $\text{Ge}_{1-x}\text{Cr}_x\text{Te}$ samples with $x \leq 0.055$. However, in the
 88 case of the samples with the highest studied compositions, i.e. $x > 0.055$, some evidence of
 89 imperfect Cr dilution was observed (see Fig. 1). Detailed measurements showed a presence of
 90 $\text{Ge}_{1-x}\text{Cr}_x\text{Te}$ accumulations with a chromium content varying in the range of $x \approx 0.40 \pm 0.05$
 91 and a diameter of around 20-30 μm , diluted randomly inside the host lattice. It is highly
 92 probable, that these accumulations can affect the magnetic properties of $\text{Ge}_{1-x}\text{Cr}_x\text{Te}$ alloys
 93 with $x > 0.055$.

95 The electrical properties of $\text{Ge}_{1-x}\text{Cr}_x\text{Te}$ alloy were studied via resistivity and the Hall
 96 effect measurements performed at temperatures between 4.3 and 300 K. We used a standard
 97 6-contact dc current technique. The Hall effect measurements were done using a constant
 98 magnetic field $B = 1.4$ T. The results of electrical characterization of the samples obtained
 99 at room temperature are gathered in Table I. The temperature dependent resistivity shows
 100 a behavior typical of a degenerate semiconductor, i.e. a metallic, nearly linear behavior of
 101 $\rho_{xx}(T)$ at $T > 30$ K and a plateau for $T < 30$ K. The data gathered in Table I indicate a
 102 decrease in ρ_{xx} value at room temperature with addition of chromium to the alloy. It might
 103 indicate that the carrier transport was strongly influenced by the addition of Cr ions into

104 the alloy. However, more clear conclusions can be stated from the analysis of the Hall effect
 105 data (see Table I). The results showed that all the studied $\text{Ge}_{1-x}\text{Cr}_x\text{Te}$ crystals had a high p -
 106 type conductivity with relatively high carrier concentrations $n \approx 2...4 \times 10^{20} \text{ cm}^{-3}$. The data
 107 gathered in Table I show that the Hall carrier concentration, n , is an increasing function of Cr
 108 content x . It is a clear signature, that some chromium ions do not substitute in cation lattice
 109 sites in GeTe host lattice, remaining in a different charge state than the Cr^{2+} state. It is
 110 probable, that a small fraction of chromium ions remains as interstitial defects in the studied
 111 crystals. This may result in a change of a charge state of chromium and allows these ions to
 112 be electrically active. The Hall carrier mobility μ , determined using a relation $\sigma_{xx} = e \cdot n \cdot \mu$,
 113 where e is the elementary charge, is also an increasing function of chromium content x up
 114 to $x = 0.059$ (see Table I). The simultaneous increase of the Hall carrier concentration n and
 115 mobility μ with increasing chromium content x must be of a complex origin. The main source
 116 of high p -type conductivity in IV-VI semiconductors is cation vacancies.²⁴ We believe that
 117 the increasing $n(x)$ dependence was not originating from imperfect distribution of dopants
 118 in the semiconductor matrix. Probably, addition of chromium to the alloy changes slightly
 119 the thermodynamics of growth by inducing an increasing number of cation vacancies in the
 120 as grown crystals and thus leading to an increasing $n(x)$ function. On the other hand, the
 121 increasing $\mu(x)$ function must be connected with some weakening of the ionic scattering
 122 mechanism related to the negative charge state of Ge vacancies in GeTe. Thus, it is highly
 123 probable, that interstitial chromium ions are associated with Ge vacancies, screening their
 124 Coulomb potential and reducing their effective scattering cross-section. It seems that the
 125 addition of chromium ions to the GeTe matrix is an effective way to increase the mean
 126 free path of the conducting carriers, which can be a crucial factor when analyzing magnetic
 127 properties of the samples in question.

128 III. RESULTS AND DISCUSSION

129 The detailed studies of magnetic properties of $\text{Ge}_{1-x}\text{Cr}_x\text{Te}$ crystals were performed includ-
 130 ing measurements of both static and dynamic magnetometry with the use of a LakeShore
 131 7229 susceptometer/magnetometer and a Quantum Design superconducting quantum in-
 132 terference device (SQUID) MPMS XL-7 magnetometer system. The very same pieces of
 133 $\text{Ge}_{1-x}\text{Cr}_x\text{Te}$ samples, that were previously characterized by means of magnetotransport

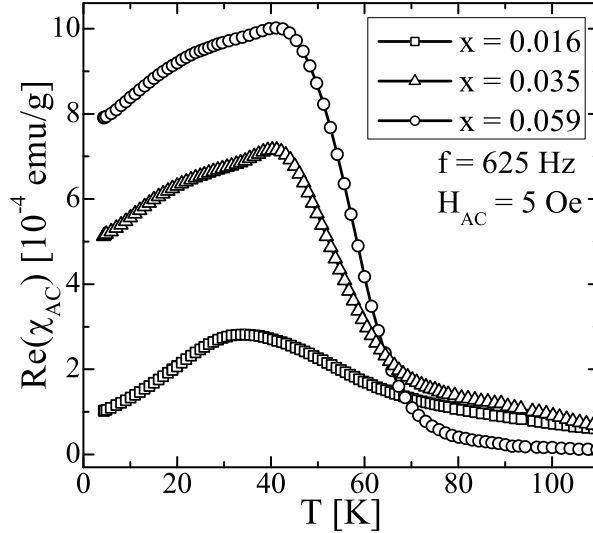


FIG. 2. The temperature dependence of the real part of the ac magnetic susceptibility χ_{AC} obtained for selected $\text{Ge}_{1-x}\text{Cr}_x\text{Te}$ samples with different chemical composition x (shown in legend).

134 measurements, with their electrical contacts removed, have been studied via several mag-
 135 netometric methods. The SQUID magnetometer was used for determining the temperature
 136 dependencies of low-field magnetization and the Lake Shore 7229 dc magnetometer was used
 137 for measurements of high field isothermal magnetization curves.

138 III.1. Low field results

139 The mutual inductance method employed in the LakeShore 7229 ac susceptometer system
 140 was used in order to measure the temperature dependence of both the real and imaginary
 141 parts of the ac susceptibility χ_{AC} . The ac susceptibility was studied at temperatures in
 142 the range of $4.3 \leq T \leq 200$ K using an alternating magnetic field with amplitudes between
 143 $1 \leq H_{AC} \leq 20$ Oe and frequencies between $7 \leq f \leq 9980$ Hz. The real and imaginary parts
 144 of the susceptibility were measured as a function of temperature using a constant frequency
 145 $f = 625$ Hz and an applied magnetic field amplitude $H_{AC} = 5$ Oe. The results of the temper-
 146 ature dependent ac susceptibility measurements are presented in Fig. 2. The $\text{Re}(\chi_{AC}(T))$
 148 curves for the samples with low chromium content, $x < 0.03$, showed a broad peak with
 149 a maximum at temperatures lower than 35 K. Peaks in the ac susceptibility shifted with
 150 frequency, as reported in Ref. 16, and were convincingly identified as the appearance of a
 151 spin-glass freezing for $x < 0.03$. However, a qualitatively different shape of the $\text{Re}(\chi_{AC}(T))$

152 curves was observed for $\text{Ge}_{1-x}\text{Cr}_x\text{Te}$ samples with $x > 0.03$. A significant increase of the
 153 $\text{Re}(\chi_{AC}(T))$ dependence as the temperature was lowered below 80 K was followed by a
 154 maximum. We believe that this is a signature that a well-defined magnetic phase transition
 155 occurred in these samples. The increase was much smaller for samples with $x < 0.03$. More-
 156 over, in contrast to the $\text{Re}(\chi_{AC}(T))$ dependence for samples with $x < 0.03$, the magnetic
 157 susceptibility was not decreasing significantly with temperatures lower than the tempera-
 158 ture for maximum χ . This is a signature that spontaneous magnetization appeared in the
 159 studied samples with $x > 0.03$ at temperatures lower than 60 K. In contrast to spin-glass
 160 samples, no signatures of frequency shifting of the maxima in the $\text{Re}(\chi_{AC}(T))$ curves with
 161 increasing frequency of the ac magnetic field were observed. It is obvious, that a ferromag-
 162 netic order was observed in the case of $\text{Ge}_{1-x}\text{Cr}_x\text{Te}$ samples with high chromium content
 163 $x > 0.03$. However, more detailed studies of static magnetic properties need to be obtained
 164 in order to fully justify the above interpretation.

165 The dc magnetometry was also used to study magnetization M vs. T of the $\text{Ge}_{1-x}\text{Cr}_x\text{Te}$
 166 crystals. At first, the temperature dependence of the magnetization was measured in the
 167 range of low magnetic field $H = 20\text{--}200$ Oe using a SQUID magnetometer. Measurements
 168 were performed over wide temperature range $T = 2\text{--}300$ K in two steps, i.e. with the sample
 169 cooled in the presence (FC) and the absence (ZFC) of the external magnetic field. The contri-
 170 bution of the sample holder was subtracted from the experimental data. The results showed
 171 that in the range of magnetic fields we used the isothermal magnetization $M(H)$ curves
 172 were nearly linear allowing us to calculate the dc magnetic susceptibility $\chi_{dc} = \partial M / \partial H$ and
 173 its changes with temperature for each $\text{Ge}_{1-x}\text{Cr}_x\text{Te}$ sample. The temperature dependence of
 174 both ZFC and FC magnetic susceptibility for a few selected samples with different chemical
 175 content x are gathered in Fig. 3. The ZFC $\chi_{dc}(T)$ curves showed different behavior in the
 176 case of $\text{Ge}_{1-x}\text{Cr}_x\text{Te}$ samples with low ($x < 0.03$) and high ($0.03 < x < 0.062$) chromium con-
 177 tent, in agreement with the previously measured ac susceptibility. It should be noted, that
 178 in the case of spin-glass samples ($x < 0.03$) the ZFC $\chi_{dc}(T)$ curve may be approximated to
 179 zero for $T \rightarrow 0$. In the case of ferromagnetic samples ($x > 0.03$) the separation between ZFC
 180 and FC curves was a decreasing function of chromium content. The features presented above
 181 are additional proofs, consistent with the ac susceptibility results, that spin-glass ($x < 0.03$)
 182 and ferromagnetic ($x > 0.03$) magnetic order was observed in the case of the studied alloy.

184 The critical behavior of the temperature dependencies of ZFC $M(T)$ curves is used to

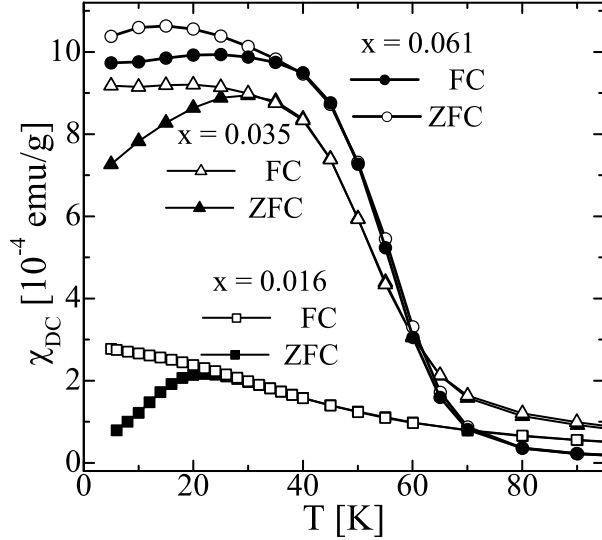


FIG. 3. The zero-field-cooled (ZFC) and field-cooled (FC) dc magnetic susceptibility as a function of temperature for selected $\text{Ge}_{1-x}\text{Cr}_x\text{Te}$ crystals with different Cr content x (see labels).

185 determine the Curie temperature, T_C , for each of the studied $\text{Ge}_{1-x}\text{Cr}_x\text{Te}$ samples. We
 186 determined the values of T_C from the position of the inflection point on the low-field magne-
 187 tization curves, $M(T)$. The values of the estimated critical temperatures for all the studied
 188 $\text{Ge}_{1-x}\text{Cr}_x\text{Te}$ samples, including our earlier estimations of the spin-glass transition tempera-
 189 tures T_{SG} for samples with $x < 0.026$ (see Ref. 16) are gathered in Fig. 4. It should be noted,
 190 that the values of both T_{SG} and T_C estimated from the dynamic susceptibility results were
 192 close to those estimated with the use of static magnetization results. The results presented
 193 in Fig. 4 show clearly the monotonic increase of the critical temperature of the alloy with the
 194 increase in the chromium concentration for $0.016 \leq x \leq 0.045$. The monotonic increase of the
 195 critical temperature with x for the samples showing both spin-glasslike and ferromagnetic
 196 ordering substantiates the assumption that both types of magnetic order originated from a
 197 single type of long range RKKY magnetic interactions. Long range RKKY magnetic inter-
 198 actions promote an appearance of a spin-glass state at low paramagnetic ions content. It is
 199 connected with the similar probability of finding two spins with both positive and negative
 200 sign of the exchange constant at low dilution limit. Due to this probability, the appearance
 201 of a spin-glass state is expected for $0.016 \leq x \leq 0.025$. The increase of chromium amount in-
 202 creases the probability of magnetic interactions with positive sign of the exchange constant.
 203 This results in an appearance of a ferromagnetic state in $\text{Ge}_{1-x}\text{Cr}_x\text{Te}$ samples for $x \geq 0.035$.

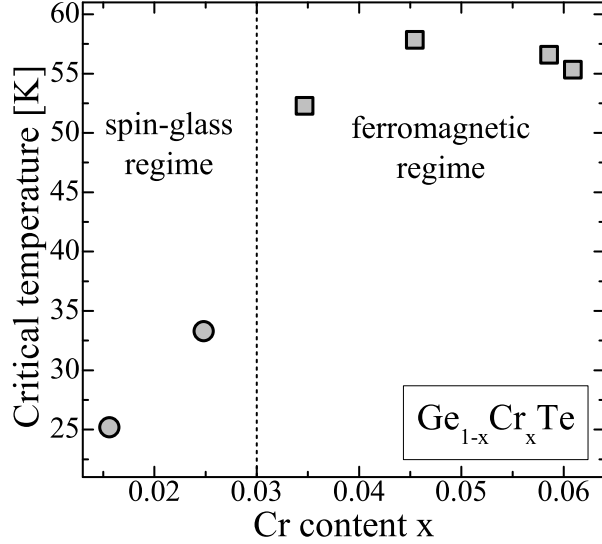


FIG. 4. The critical temperatures as a function of Cr content x for the studied $\text{Ge}_{1-x}\text{Cr}_x\text{Te}$ samples.

204 III.2. High field magnetization

205 The magnetic behavior of the $\text{Ge}_{1-x}\text{Cr}_x\text{Te}$ samples was investigated with the use of mag-
 206 netization M measurements in the presence of a dc magnetic field up to $H = 90$ kOe. We
 207 used the Weiss extraction method included in the LakeShore 7229 magnetometer system. At
 208 first, detailed isothermal magnetic hysteresis loops were measured at selected temperatures
 209 $T < 200$ K. A clear magnetic hysteresis was observed in all the studied crystals at temper-
 210 atures lower than either T_{SG} or T_C . It should be emphasized, that a hysteretic behavior
 211 was observed in both the spin-glass and the ferromagnetic regime of the studied alloy (see
 212 Fig. 5). The appearance of a well defined hysteretic behavior in a spin-glass system is a
 213 signature that a strong magnetic disorder is causing significant magnetic frustration in the
 214 samples with $x < 0.03$. Such a feature was observed in many representatives of metallic
 215 spin-glasses such as AuFe with 8 at.% Fe (Ref. 25) or NiMn with 21 at.% Mn (Ref. 26).
 216

217 A series of magnetic hysteresis loops obtained at temperatures $T < 100$ K was used to
 218 determine the temperature dependencies of both coercive field H_C and spontaneous mag-
 219 netization M_R (see the right panel of Fig. 5). The H_C observed at $T = 4.5$ K changed
 220 monotonically as a function of x indicating that large changes in the domain structure of
 221 the studied system occurred while changing its chemical composition. It is especially visible
 222 in the case of the $H_C(x)$ dependence, where we observed differences higher than an order
 223 of magnitude; H_C depended on the temperature and at 4.5 K was 800 Oe for $x = 0.016$

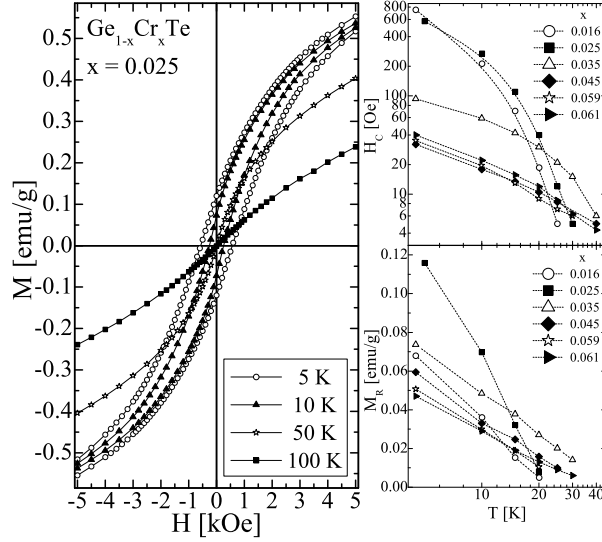


FIG. 5. Magnetic hysteresis curves obtained at different temperatures for the $\text{Ge}_{0.975}\text{Cr}_{0.025}\text{Te}$ sample (left panel) together with temperature dependence of coercive field H_C and spontaneous magnetization M_R (right panel).

224 and 40 Oe for $x = 0.061$. The trend in the M_R with x had more complicated character first
 225 increasing for $x \leq 0.025$ and then decreasing as a function of x .

226 The high-field isothermal magnetization curves were studied in the case of all the
 227 $\text{Ge}_{1-x}\text{Cr}_x\text{Te}$ samples at $H \leq 90$ kOe and $T < 200$ K. In order to compare the results we
 228 plotted $M(H)$ curves measured at the lowest measurement temperature $T = 4.5$ K for the
 229 samples having different chemical composition (see Fig. 6). As we can see, the magnetiza-
 230 tion curves have different shapes for samples showing spin-glass ordering ($x < 0.03$) than for
 231 the ferromagnetic ones ($x > 0.03$). The $M(H)$ curves in the case of the spin-glass samples
 232 saturated slowly and even at high magnetic fields $H = 90$ kOe, did not reach the saturation.
 233 In case of ferromagnetic crystals the magnetization reached a saturation value for magnetic
 234 fields below 20 kOe. It should be noted, that for the samples with $x > 0.03$ the magnetization
 235 is slowly decreasing as a function of magnetic field for $H > 30$ kOe. This is a diamagnetic
 236 contribution from the GeTe lattice.
 237

238 The saturation magnetization $M_S(T = 4.5 \text{ K})$ was an increasing function of Cr content for
 239 $x < 0.05$, and showed a small decrease for higher x . The amount of the magnetically active Cr
 240 ions in the material can be determined from the value of the saturation magnetization, M_S
 241 observed at $T = 4.5$ K. We use the typical formula describing the saturation magnetization

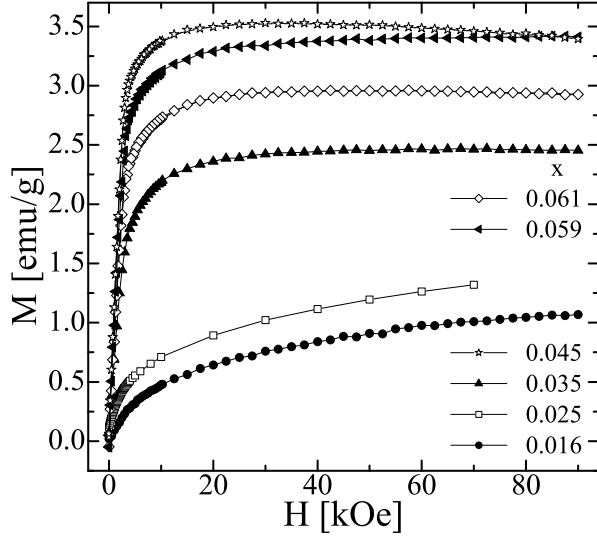


FIG. 6. High field magnetization curves obtained at $T = 4.5$ K for the studied $\text{Ge}_{0.975}\text{Cr}_{0.025}\text{Te}$ samples with different chromium content x .

242 for the calculation of the amount of Cr in the studied compound, $\bar{x} = (M_S m_u) / (N_{Av} g J \mu_B)$,
 243 where m_u is the particle mass of the $\text{Ge}_{1-x}\text{Cr}_x\text{Te}$ alloy, N_{Av} is the Avogadro constant, g is
 244 the effective spin splitting factor, $J = S = 2$ is the total momentum of the Cr^{2+} ion, and μ_B is
 245 the Bohr magneton. The \bar{x} estimation assumes that the spin-component of the momentum
 246 $S = 2$ in the GeTe crystal field. The obtained values of \bar{x} are about 2-times lower than
 247 the values obtained using the EDXRF method indicating, that half of the Cr ions in the
 248 alloy are magnetically inactive. It is also possible that some Cr ions are in the Cr^{3+} state,
 249 with $J = S = 3/2$. Let us also mention that for purely random, uncorrelated distribution of
 250 substitutional Cr ions, some fraction of them forms clusters, in which nearest-neighbor ions
 251 couple antiferromagnetically due to superexchange mechanism.

252 III.3. Estimation of the exchange integral J_{pd}

253 In order to gain more insight into the physical mechanism behind the magnetic order-
 254 ing in the samples with low Cr content $x = 0.016$ and 0.025 (where the Cr distribution is
 255 homogeneous and no spinodal decomposition was observed), SQUID measurements of the
 256 temperature dependence of magnetization in weak external fields of 20, 50, 100 and 200 Oe
 257 were performed. The results for the sample with $x = 0.025$ are presented in Fig. 7. Our
 258 interest was particularly focused on examining whether the Bloch law for magnetization is

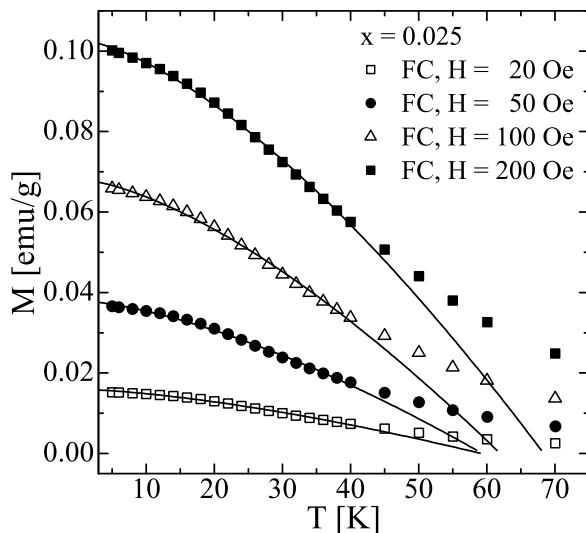


FIG. 7. The temperature dependence of the FC magnetization obtained experimentally (symbols) and calculated (lines) for different magnetic field values (see legend) for the $\text{Ge}_{0.975}\text{Cr}_{0.025}\text{Te}$ sample.

259 fulfilled in the form $M(T) = M(0) \left[1 - (T/T_{SW})^{3/2} \right]$. The parameter T_{SW} is related to
 260 the spin-wave stiffness D by $T_{SW} = \frac{4\pi D}{k_B a^2} \left(\frac{4J}{\zeta(3/2)} \right)^{2/3}$, where a is the lattice constant and
 261 $\zeta(3/2) \simeq 2.612$ is the appropriate Riemann zeta function, while $J=2$ is the ionic angular
 262 momentum.^{6,23} Spin wave stiffness is defined by the relation between spin wave energy E and
 263 wavevector q of the form $E = Dq^2$. The results of fitting the formula to the low-temperature
 264 part of the experimental data (excluding the range showing a 'magnetization tail') are shown
 265 in Fig. 7 with solid lines. It can be observed that the temperature behavior of magnetiza-
 266 tion follows very well the $T^{3/2}$ -dependence, for all the values of low external field. What is
 267 important is that the characteristic temperatures T_{SW} determined from the fittings exhibit
 268 rather weak dependence on the external field, especially for $H = 20$ and 50 Oe. Therefore,
 269 we accept the average value of T_{SW} determined for these two weakest external fields as a
 270 measure of the spin-wave stiffness. For $x = 0.016$ we obtained $T_{SW} = 53.5$ K (which corre-
 271 sponds to $D = 6.2 \text{ meV} \cdot \text{\AA}^2$), while for $x = 0.025$ $T_{SW} = 59.3$ K (yielding $D = 6.9 \text{ meV} \cdot \text{\AA}^2$).
 272

273 We attempted to apply the RKKY model to reproduce the experimental values of T_{SW} .
 274 Within the harmonic spin-wave and virtual crystal approximation, $D = \frac{1}{6} \bar{x} J \sum_i J_{RKKY}(R_{0i}) R_{0i}^2$,
 275 where summation is performed over all the lattice sites i , i.e. over all possible positions of
 276 substitutional magnetic impurity ions, relative to a selected lattice site denoted by 0.²³ Let
 277 us note that instead of the EDXRF-measured Cr content x we use the \bar{x} values, estimated

278 from the low-temperature high-field magnetization (see previous section). We expect that
 279 only this magnetically active fraction of Cr ions participates in spin wave excitations in the
 280 system. The values amount to $\bar{x} = 0.0096$ for the sample with $x = 0.016$ and $\bar{x} = 0.013$ for
 281 $x = 0.025$, respectively. The indirect RKKY exchange integral between a pair of magnetic
 282 ions at lattice sites 0 and i with the relative distance R_{0i} equals¹⁷⁻¹⁹

$$J_{RKKY}(R_{0i}) = N_V \frac{m^* J_{pd}^2 a^6 k_F^4}{32\pi^3 \hbar^2} \times \frac{\sin(2k_F R_{0i}) - 2k_F R_{0i} \cos(2k_F R_{0i})}{(2k_F R_{0i})^4} \exp\left(-\frac{R_{0i}}{\lambda}\right), \quad (1)$$

283 where m^* is the effective mass of the carriers residing in $N_v = 4$ valleys in the valence band,
 284 J_{pd} is the exchange integral between charge carriers and Cr ions, while $k_F = (3\pi^2 n/N_V)$
 285 denotes the Fermi wave vector.

286 In order to account for the presence of a disorder and a finite mean free path of the
 287 charge carriers mediating the RKKY coupling we assume an exponential damping with a
 288 length scale λ . We estimated the values of λ on the basis of the Drude model of conduction
 289 taking into account the experimentally observed low-temperature values of the Hall carrier
 290 concentration and mobility. Knowing the values of charge carriers concentration for $T \rightarrow 0$
 291 as well as the mobility μ , we can calculate the mean free path as $\lambda = (\hbar k_F \mu) / e$. For the
 292 sample with $x = 0.016$ we obtained $\lambda = 9.5 \text{ \AA}$, while for $x = 0.025$ we obtained $\lambda = 12.5 \text{ \AA}$.
 293 We use these estimates for the RKKY-based model of spin-wave stiffness.

294 Under such assumptions, we are able to reproduce the experimental values of T_{SW} using
 295 $J_{pd} = 0.88 \pm 0.05 \text{ eV}$ for $x = 0.016$ and $J_{pd} = 0.77 \pm 0.05 \text{ eV}$ for $x = 0.025$. The obtained esti-
 296 mates are close to each other, within the experimental uncertainty, including the uncertainty
 297 in determination of the magnetically active Cr concentration in the samples, \bar{x} .

298 IV. SUMMARY AND CONCLUSIONS

299 We presented detailed studies of magnetic properties of $\text{Ge}_{1-x}\text{Cr}_x\text{Te}$ bulk crystals grown
 300 using the modified Bridgman method with chromium content changing in the range of
 301 $0.016 \leq x \leq 0.061$. The X-ray diffraction studies revealed that a Vegard law was fulfilled in
 302 the alloy indicating a proper solubility of chromium in the crystal lattice. All the studied
 303 samples were p -type semiconductors with high carrier concentrations $n \approx 2.4 \dots 3.3 \times 10^{20} \text{ cm}^{-3}$
 304 and mobilities $\mu \approx 8 \dots 23 \text{ cm}^2 / (\text{Vs})$.

305 The magnetic properties of the $\text{Ge}_{1-x}\text{Cr}_x\text{Te}$ are composition dependent. The presence of
306 spin-glass and ferromagnetic phase was observed at $T < 60$ K, for the samples with $x < 0.03$
307 and $x \geq 0.03$, respectively. The RKKY interactions are found to be responsible for the
308 observed magnetic ordering for $x < 0.045$, while for $x \geq 0.045$ the spinodal decomposition
309 of Cr ions leads to saturation and decrease of the Curie temperature, T_C , with increasing
310 x . The hysteretic behavior was observed both for spin-glass and ferromagnetic samples at
311 $T < 50$ K with strong composition dependencies of the coercive field H_C . The amount of
312 magnetically active Cr ions, \bar{x} , estimated from the value of the saturation magnetization
313 M_S , was about 2-times lower than the value of the Cr content x obtained using the EDXRF
314 method. The calculations based on spin waves model reproduced the observed magnetic
315 properties of the alloy for $x < 0.04$ and proved, that carrier mediated RKKY interaction is
316 responsible for the observed magnetic states. The value of the Cr-hole exchange integral
317 J_{pd} , estimated via fitting of the experimental results with the theoretical model was about
318 0.77 eV for $x = 0.025$ and 0.88 eV for $x = 0.016$.

319 V. ACKNOWLEDGMENTS

320 Scientific work was financed from funds for science in 2009-2013, under the project no.
321 IP2010017770 granted by Ministry of Science and Higher Education of Poland and project
322 no. NN202 166840 granted by National Center for Science of Poland. This work has been
323 partly supported by the Foundation for Polish Science under the project POMOST/2011-
324 4/2.

325 This work has been partly supported by Polish Ministry of Science and Higher Educa-
326 tion by a special purpose grant to fund the research and development activities and tasks
327 associated with them, serving the development of young scientists and graduate students.

328 REFERENCES

- 329 ¹H. Ohno, *Nature Materials* **9**, 952 (2010).
330 ²T. Dietl, *Nature Materials* **9**, 965 (2010).
331 ³J. Kossut and W. Dobrowolski, *Handbook of Magnetic Materials* (North-Holland, Ams-
332 terdam, 1993), Vol. 7, pp. 231.

- 333 ⁴F. Matsukura, H. Ohno, and T. Dietl, Handbook of Magnetic Materials (Elsevier, Amsterdam, 2002), Vol. 14, Chaps. III–V, pp. 1.
- 334
- 335 ⁵W. Dobrowolski, J. Kossut, and T. Story, Handbook of Magnetic Materials (Elsevier, New York, 2003), Vol. 15, Chaps. II–VI and IV–VI, pp. 289.
- 336
- 337 ⁶R. W. Cochrane, M. Plishke, and J. O. Ström-Olsen, *Phys. Rev. B* **9**, 3013 (1974).
- 338 ⁷M. Hassan, G. Springholz, R. T. Lechner, H. Groiss, R. Kirchschrager, and G. Bauer, *J. Cryst. Growth* **323**, 363 (2011).
- 339
- 340 ⁸W. Knoff, V. Domukhovski, K. Dybko, P. Dziawa, R. Jakiela, E. Łusakowska, A. Reszka, K. Świątek, B. Taliashvili, T. Story, K. Szalowski, and T. Balcerzak, *Acta Phys. Pol. A* **116**, 904 (2009).
- 341
- 342
- 343 ⁹Y. Fukuma, H. Asada, S. Miyawaki, T. Koyanagi, S. Senba, K. Goto, and H. Sato, *Appl. Phys. Lett.* **93**, 252502 (2008).
- 344
- 345 ¹⁰R. T. Lechner, G. Springholz, M. Hassan, H. Groiss, R. Kirchschrager, J. Stangl, N. Hrauda, and G. Bauer, *Appl. Phys. Lett.* **97**, 023101 (2010).
- 346
- 347 ¹¹Y. Fukuma, H. Asada, J. Miyashita, N. Nishimura, and T. Koyanagi, *J. Appl. Phys.* **93**, 7667 (2003).
- 348
- 349 ¹²Y. Fukuma, N. Nishimura, F. Odawara, H. Asada, and T. Koyanagi, *J. Supercond. Nov. Magn.* **16**, 71 (2003).
- 350
- 351 ¹³Y. Fukuma, Y. H. Asada, T. Taya, T. Irida, and T. Koyanagi, *Appl. Phys. Lett.* **89**, 152506 (2006).
- 352
- 353 ¹⁴Y. Fukuma, Yamaguchi T. Taya, S. Miyawaki, T. Irida, H. Asada, and T. Koyanagi, *J. Appl. Phys.* **99**, 08D508 (2006).
- 354
- 355 ¹⁵Y. Fukuma, H. Asada, N. Moritake, T. Irida, and T. Koyanagi, *Appl. Phys. Lett.* **91**, 092501 (2007).
- 356
- 357 ¹⁶L. Kilanski, M. Górska, W. Dobrowolski, M. Arciszewska, V. Domukhovski, J. R. Anderson, N. P. Butch, A. Podgórní V. E. Slynko, and E. I. Slynko, *Acta Phys. Pol. A* **119**, 654 (2011).
- 358
- 359
- 360 ¹⁷M. A. Ruderman, C. Kittel, *Phys. Rev.* **96**, 99 (1954).
- 361 ¹⁸T. Kasuya, *Progr. Theor. Phys.* **16**, 45 (1956).
- 362 ¹⁹K. Yoshida, *Phys. Rev.* **106**, 893 (1957).
- 363 ²⁰K. T. Aust and B. Chalmers, *Can. J. Phys.* **36**, 977 (1958).

- 364 ²¹R. R. Galazka, J. Kossut, and T. Story, Semiconductors, Landolt–Börnstein, New Series,
365 Group III, Vol. 41, edited by U. Rössler (Springer-Verlag, Berlin, Heidelberg, 1999).
- 366 ²²Y. Fukuma, H. Asada, N. Nishimura, and T. Koyanagi, *J. Appl. Phys.* **93**, 4034 (2003).
- 367 ²³L. Kilanski, R. Szymczak, W. Dobrowolski, K. Szałowski, V. E. Slynko, E. I. Slynko, *Phys.*
368 *Rev. B* **82**, 094427 (2010).
- 369 ²⁴R. W. Ure, J. R. Bowers, and R. C. Miller. In Properties of Elemental and Compound
370 Semiconductors, Metallurgical Society Conferences Vol. 5, page 254. New York, London:
371 Interscience Publishers, 1960.
- 372 ²⁵J. J. Prejean, M. J. Joliclerc, and P. Monod, *J. Phys. (Paris)* **41**, 427 (1980).
- 373 ²⁶S. Senoussi, *J. Phys. (Paris)* **45**, 315 (1984).